

# PROCEEDINGS OF SPIE

[SPIDigitalLibrary.org/conference-proceedings-of-spie](https://SPIDigitalLibrary.org/conference-proceedings-of-spie)

## Effects of iron-oxide nanoparticles and magnetic fields on oral biofilms

Gema Alas, Ronald Pagano, Jane Nguyen, H. M. H. Nihal Bandara, Sergei Ivanov, et al.

Gema Alas, Ronald E. Pagano, Jane Q. Nguyen, H. M. H. Nihal Bandara, Sergei A. Ivanov, Gennady A. Smolyakov, Dale L. Huber, Hugh D. C. Smyth, Marek Osiński, "Effects of iron-oxide nanoparticles and magnetic fields on oral biofilms," Proc. SPIE 10078, Colloidal Nanoparticles for Biomedical Applications XII, 1007806 (22 February 2017); doi: 10.1117/12.2256221

**SPIE.**

Event: SPIE BiOS, 2017, San Francisco, California, United States

# Effects of iron-oxide nanoparticles and magnetic fields on oral biofilms

Gema Alas<sup>1</sup>, Ronald E. Pagano<sup>1</sup>, Jane Q. Nguyen<sup>1</sup>, H. M. H. Nihal Bandara<sup>2</sup>, Sergei A. Ivanov<sup>3</sup>,  
Gennady A. Smolyakov<sup>1</sup>, Dale L. Huber<sup>4</sup>, Hugh D. C. Smyth<sup>5</sup>, and Marek Osiński<sup>1</sup>

<sup>1</sup>Center for High Technology Materials, University of New Mexico, 1313 Goddard St. SE,  
Albuquerque, NM 87106-4343, USA

<sup>2</sup>Department of Health and Behavioral Sciences, School of Dentistry, University of Queensland,  
Herston Road, Herston 4006, Brisbane, Australia

<sup>3</sup>Center for Integrated Nanotechnologies, Los Alamos National Laboratory, 1000 Eubank SE,  
Albuquerque, New Mexico 87123, USA

<sup>4</sup>Center for Integrated Nanotechnologies, Sandia National Laboratories, 1000 Eubank SE,  
Albuquerque, New Mexico 87123, USA

<sup>5</sup>College of Pharmacy, University of Texas at Austin, 2409 University Avenue, Stop A1900,  
Austin, TX 78712, USA

## ABSTRACT

Human mouth is a host of a large gamut of bacteria species, with over 700 of different bacteria strains identified. Most of these bacterial species are harmless, some are beneficial (such as probiotics assisting in food digestion), but some are responsible for various diseases, primarily tooth decay and gum diseases such as gingivitis and periodontitis. For example, *Streptococcus mutans* produces enamel-eroding acids, while *Porphyromonas gingivalis* is strongly linked to periodontitis. In this paper, we report on the effects of exposure of oral biofilms to iron oxide nanoparticles and static magnetic fields as possible bactericidal agent.

**Keywords:** Oral biofilms; Iron oxide nanoparticles; Bactericidal effects; Magnetic field effects.

## 1. INTRODUCTION

Gingivitis and periodontitis are the most common types of adult gum disease, and may result in tooth loss. Gingivitis is an inflammation of the gums without the loss of connective tissue. It is extremely common and its main cause is poor dental hygiene. Currently, the prescribed treatment for gingivitis is fairly inadequate and is entirely dependent on the patient to simply increase vigilance towards domestic dental care. It is seemingly harmless, preventable, and reversible, but if oral hygiene habits are poor, gingivitis may progress to periodontitis. Periodontitis manifests itself in loss of bone and the collagen structures supporting the teeth. It increases risks of heart attack and stroke. It is irreversible, but its progression can be stopped by proper oral hygiene and treatment.

In 2012, data from the Center for Disease Control and Prevention estimated that 47.2% or 64.7 million of American adults are victims of periodontitis, the most dangerous and irreversible periodontal disease [Eke 2012]. This percentage increases to 70.1% of Americans aged 65 and older. Taking into account the progression of the disease, 8.7% (11.9 million) of American adults had mild periodontitis, 30% (41.1 million) had moderate periodontitis, and 8.5% (11.7 million) suffered from severe periodontitis. Most people with periodontitis are not even aware that they have the disease. The wide spread of the periodontal disease is nationally overlooked due to its commonality. This causes massive concern for future dental care practices in periodontology.

Nanoparticles (NPs) have outstanding antimicrobial abilities, but are also infamously known to cause cytotoxicity and inflammation within the human body. For example, recent study has shown that TiO<sub>2</sub> NPs can act as a successful antibacterial agent against gingival bacteria [Garcia-Contreras 2015]. However, as TiO<sub>2</sub> NPs infiltrated oral cells, they enhanced gingival inflammation. This indicates dental treatment with TiO<sub>2</sub> NPs could have negative side effects,

consistent with other reports of toxicity of TiO<sub>2</sub> NPs on blood cells [Khan 2015], [Kongseng 2016], renal system [Iavicoli 2016], lungs [Hanot-Roy 2016], [Schmid 2016], and central nervous system [Coccini 2015], [Hong 2015], [Czajka 2015], as well as their genotoxicity [Chen 2014], [Hanot-Roy 2016], [Kongseng 2016].

The poor quality of gingivitis treatment and the biomedical limitations of NPs such as TiO<sub>2</sub> indicate a need for development of nontoxic substances that have increased potency as an antimicrobial agent, but are safe enough to be used in household dental care products. Due to their biocompatibility, iron oxide NPs find an increasing number of biomedical applications. For example, they have been used as contrast agents for magnetic resonance imaging, in biosensors and targeted drug delivery, cell sorting, for cancer therapy using hyperthermia, as food preservation agents, and are FDA-approved. On the other hand, they have been demonstrated by several groups to have bactericidal activity against various species of bacteria [Tran 2010], [Behera 2012], [Prabhu 2015], [Armijo 2015], [Niemirowicz 2015]. For these reasons, we have chosen to investigate whether Fe<sub>3</sub>O<sub>4</sub> NPs can satisfy the need for a safe antimicrobial agent in oral hygiene and relieve the burden of lifetime disease management currently faced by patients with periodontitis.

### 1.1 Bactericidal Effects of Iron Oxide Nanoparticles

Numerous studies have established that properly biofunctionalized Fe<sub>3</sub>O<sub>4</sub> NPs can have bactericidal effect on *Staphylococcus aureus* [Tran 2010], [Behera 2012], [Prabhu 2015], [Darwish 2015], *Bacillus licheniformis*, *Staphylococcus epidermidis*, *Streptococcus aureus* [Behera 2012], *Bacillus subtilis* [Behera 2012], [Arakha 2015], *Escherichia coli* [Behera 2012], [Prabhu 2015], [Darwish 2015], [Arakha 2015], *Proteus vulgaris*, *Xanthomonas* [Prabhu 2015], and *Pseudomonas aeruginosa* [Armijo 2015], [Niemirowicz 2015]. The exact mechanism of the antimicrobial action of Fe<sub>3</sub>O<sub>4</sub> NPs that results in damaging the bacterial proteins and DNA has not yet been determined, but it has been hypothesized that it might involve oxidative stress caused by reactive oxygen species, such as superoxide radicals (O<sub>2</sub><sup>-</sup>), singlet oxygen (<sup>1</sup>O<sub>2</sub>), hydroxyl radicals (•OH), or hydrogen peroxide (H<sub>2</sub>O<sub>2</sub>) [Rudramurthy 2016]. For example, H<sub>2</sub>O<sub>2</sub> could penetrate the cell membrane of the bacteria and kill the bacteria by entering the intracellular space.

It has also been established that bactericidal activity of Fe<sub>3</sub>O<sub>4</sub> NPs strongly depends on the surface coating, and should be individually optimized for maximum effect on a particular bacterial species [Darwish 2015], [Arakha 2015]. For example, changing the zeta potential of as-synthesized iron oxide NPs from negative to positive by coating their surface with biocompatible chitosan has significantly increased their antimicrobial activity against Gram-positive *Bacillus subtilis* and Gram-negative *Escherichia coli*, reducing the percentage of viable cells after 22-hour exposure to 50 μM of NP suspension in nutrient broth from over 60% to less than 30% for either bacterial species [Arakha 2015]. Sensitivity to surface coating may also be a reason for large differences in results reported by various groups, as the NPs used in the experiments would often have different coatings.

### 1.2 Oral bacteria and onset of gingivitis

Human mouth is a host of a large gamut of bacteria species, with over 700 of different bacteria strains identified. The human oral microbiome includes Gram positive and Gram negative bacteria, cocci, rods, filaments, spirochetes, etc. Most of the oral bacteria have never been cultured. Some of these bacteria belong to very exotic taxonomic groups, for example Archea that are found in termite guts and other extreme environments. Most of these bacterial species are harmless, some are beneficial (such as probiotics assisting in food digestion), but some are responsible for various diseases, primarily tooth decay and gum diseases such as gingivitis and periodontitis. For example, *Streptococcus mutans* produces enamel-eroding acids, while *Porphyromonas gingivalis* is strongly linked to periodontitis. Together with the bacteria, there are also fungi and viruses.

Bacteria colonize a variety of surfaces in human mouth. Bacterial biofilms on tooth surfaces are known as dental plaque. It consists of at least 800 different bacterial species, and already in 2010 this number was expected to rise into the thousands with the advances in mass sequencing techniques [Filoche 2010]. Indeed, as of February 2016, the Human Oral Microbiome Database listed 1,200 predominant oral bacteria species, with some 19,000 phylotypes and with distinct subsets predominating in different habitats [Carrouel 2016].

Oral biofilms develop under a range of different conditions and various environments. In particular, dental plaque is a dynamic and extremely complex oral biofilm ecosystem. It is a structured multi-species community embedded in a matrix with water channels, with four distinct stages of development: attachment, growth, ecological succession, and maturation. Factors that affect dental plaque development include interbacterial co-adhesion, pH, level of oxygen, and availability of various nutrients. The microbial species in dental plaque form complex communities, with an assortment of micro-niches, metabolic functions, and inter- and intra-species interactions.

Development of dental plaque proceeds in three stages [Kolenbrander 2002]. Initially, Gram-positive early colonizers (*Streptococcus gordonii*, *Streptococcus mitis*, *Streptococcus oralis*, *Streptococcus sanguis*) bind via adhesins to complementary receptors in the acquired pellicle of saliva proteins coating the tooth surface. Then, Gram-negative secondary colonizers (*Fusobacterium nucleatum*) bind to previously bound primary colonizers, and provide a bridge through which a large group of late colonizers (*Actinobacillus actinomycetemcomitans*, *Actinomyces israelii*, *Actinomyces naeslundii*, *Capnocytophaga gingivalis*, *Capnocytophaga ochracea*, *Capnocytophaga sputigena*, *Eikenella corrodens*, *Eubacterium* spp, *Porphyromonas gingivalis*, *Prevotella denticola*, *Prevotella intermedia*, *Prevotella loescheii*, *Propionibacterium acnes*, *Selenomonas flueggei*, *Treponema denticola*, *Veillonella atypica*) can access the biofilm. Sequential binding of late colonizers results in the appearance of nascent surfaces that bridge with the next coaggregating partner cells.

## 2. SYNTHESIS AND CHARACTERIZATION OF $\text{Fe}_3\text{O}_4$ NANOPARTICLES

### 2.1 Synthesis of $\text{Fe}_3\text{O}_4$ Nanoparticles

Numerous different approaches are available for the synthesis of  $\text{Fe}_3\text{O}_4$  NPs, including co-precipitation, solvothermal or hydrothermal processing, sol-gel and forced hydrolysis, microemulsion processing, surfactant-mediated synthesis, laser pyrolysis, and electrochemical processing. We have chosen a solvothermal method that involves pyrolysis of iron (III) acetylacetonate ( $\text{Fe}(\text{acac})_3$ ) in high-boiling-point triethylene glycol (TREG) solvent, as it directly produces biocompatible water-soluble nanoparticles with a very high reaction yield. TREG plays a triple role of a solvent, reducing agent, and modifying agent in the reaction. The melting point of  $\text{Fe}(\text{acac})_3$  of 180-181 °C coincides with the onset of its thermal decomposition [Von Hoene 1958].

In our synthesis,  $\text{Fe}(\text{acac})_3$  dissolved in TREG was used as a precursor, resulting in highly crystalline magnetite ( $\text{Fe}_3\text{O}_4$ ) NPs coated in TREG, with a typical size of 5-10 nm, depending on the reaction time and the ratio of  $\text{Fe}(\text{acac})_3$ /TREG. The NPs were synthesized using the procedure of [Cai 2007], modified by increasing the molar fraction of  $\text{Fe}(\text{acac})_3$ . The procedure consists of two steps: synthesis of the iron oxide NPs and the washing of the NPs in acetone. The washing procedure was taken from [Gonçalves 2010].

**2.1.1 Materials.** Iron (III) acetylacetonate ( $\text{Fe}(\text{acac})_3$ , 97%), triethylene glycol (TREG, 99%), and acetone (99.5%) were purchased from Sigma-Aldrich, USA. All chemicals were used as received without purification.

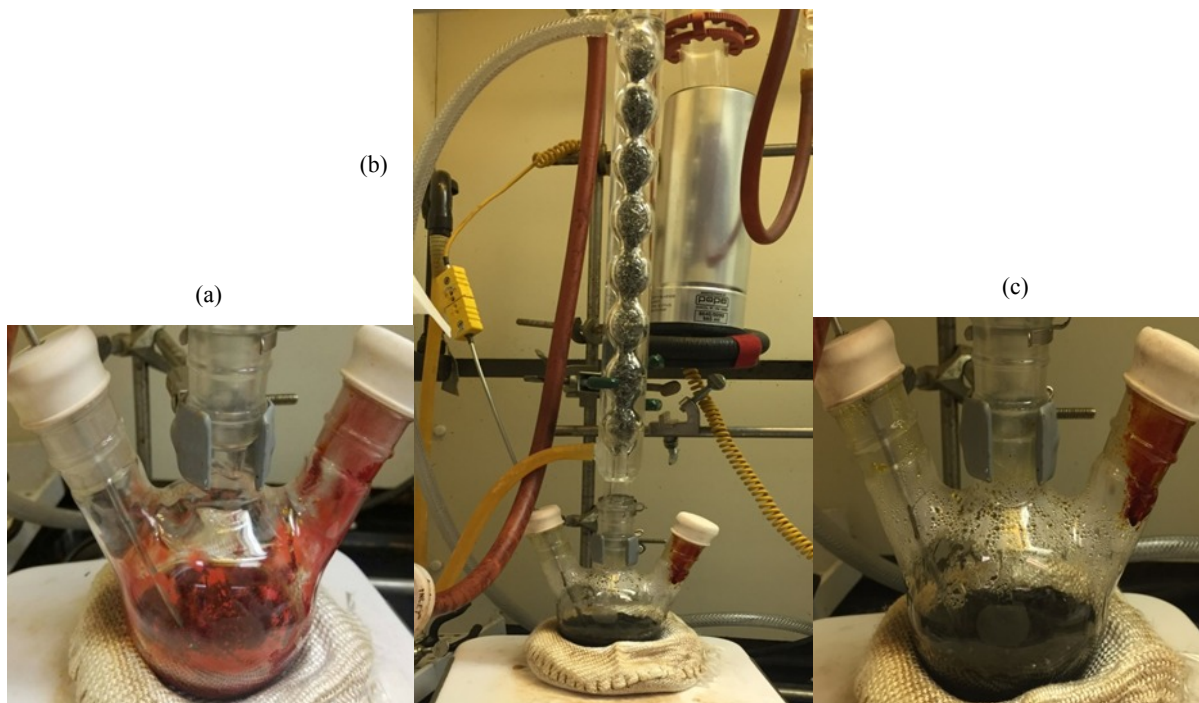


Fig. 1. (a)  $\text{Fe}(\text{acac})_3$  dissolved in TREG, prior to its pyrolysis. (b) Schlenk-line setup during the reaction, showing a condenser, a liquid nitrogen cold trap, and a thermocouple. (c) Final stage of the synthesis, with TREG refluxing during the process of NP growth.

**2.1.2 Synthesis of iron oxide (magnetite) NPs.** In a typical synthesis, 10.6 g (30 mmol) of  $\text{Fe}(\text{acac})_3$  were added to 50 mL of TREG under continuous and vigorous stirring in a 250-mL three-neck flask attached to a condenser. The condenser was connected to a Schlenk line and placed under dry nitrogen flow. The mixture was then heated to the decomposition temperature of  $\text{Fe}(\text{acac})_3$  (180 °C) at a rate of 3 °C per minute under positive nitrogen pressure with continuous and vigorous stirring. The mixture was held at 180 °C for 30 minutes. The gaseous product of pyrolysis of  $\text{Fe}(\text{acac})_3$  is mostly acetone, with a slightly increasing fraction of  $\text{CO}_2$  as the temperature is raised from 180 °C to 280 °C [Von Hoene 1958]. The temperature was then rapidly raised to the boiling point of TREG (270 °C) at rate of 10 °C per minute. The mixture was held at 270 °C for two hours, during which time the NP growth occurred, with simultaneous reflux of TREG. The TREG solvent also acted as a surfactant, forming a protective hydrophilic layer on the NP surface. After the two hours, the flask was left to cool to room temperature. The NPs were washed in acetone several times and then dried to a powder. Fig. 1 illustrates the initial and final stages of the synthesis.

**2.1.3 Washing of NPs.** The excess of TREG after the reaction was removing through multiple steps of washing in acetone. The contents of the 3-neck flask were distributed into ten 20-mL scintillation vials and topped with acetone. Ultrasonic bath was used to disperse the NPs in the vials. A tandem of 8 rare-earth arc magnets was taped to the side of each vial, and the vials were left until the liquid became light brown. The magnets were then removed and the process was repeated 2-3 times until the liquid was clear. The vials were then left open overnight to let the remaining acetone evaporate. The remaining black powder was easily dispersible in deionized water. Fig. 2 illustrates the washing process.

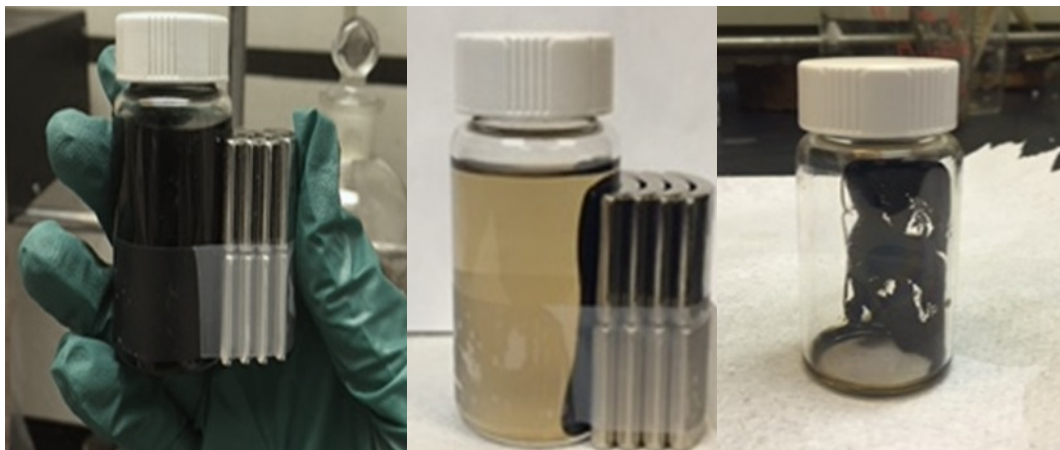


Fig. 2. (a) Appearance of scintillation vials after sonication. (b) Appearance of the vials shortly before decantation. (c) Appearance of the vials after decantation.

## 2.2 Characterization of $\text{Fe}_3\text{O}_4$ Nanoparticles

**2.2.1 Transmission electron microscopy.** For structural characterization, samples for transmission electron microscopy (TEM) were prepared by placing a drop of the colloidal solution in water onto a 200-mesh carbon-backed copper grid wetted with chlorobenzene. The liquid bilayer was allowed to evaporate away, thus fixing the NPs on the grid. High-resolution TEM (HRTEM) measurements were taken with a JEOL-2010F transmission electron microscope operating at 200 kV, with a charge-coupled device (CCD) camera attachment and equipped with an OXFORD Link ISIS/Inca energy dispersive spectroscopy (EDS) apparatus, used to determine the elemental composition of the sample.

Fig. 3 shows an example of a TEM image of as-synthesized magnetite NPs. Their average size is ~10 nm. Most NPs are spherical, although some tend to be hexagonal in shape.

Fig. 4 shows the measured EDS spectrum. The electron beam was focused on a single NP and the characteristic x-ray peaks specific to each element were identified using the OXFORD Link ISIS software. As shown in Fig. 4, the EDS spectrum confirms the presence of iron and oxygen. The carbon and copper lines are from the carbon-backed copper grid.

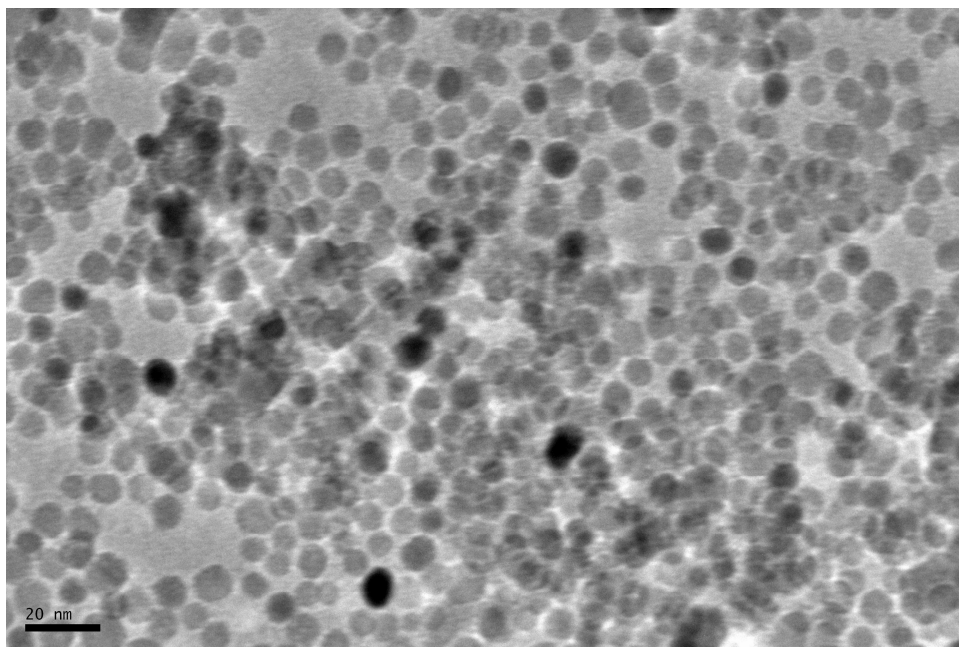


Fig. 3. TEM image of magnetite NPs. Scale bar is 20 nm.

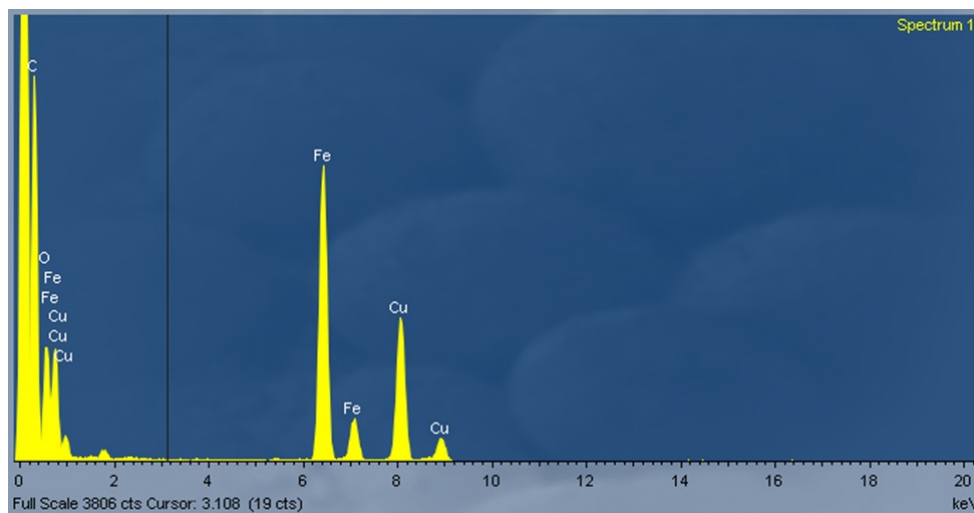


Fig. 4. EDS spectrum of magnetite NPs.

*2.2.2 Zeta potential analysis.* Zeta potential was measured using a Malvern Zetasizer Nano-Z apparatus. The zeta potential is measured by placing the sample in an electric field and measuring how fast, and in which direction the NPs move between the anode and the cathode while suspended in a liquid solvent. Using this measurement, along with the viscosity of the solvent, the Zetasizer is able to calculate the zeta potential, which is an indicator of the electrostatic stability of the NPs in a liquid. The zeta potential is the electrical potential that occurs in the interfacial double plane, which is located at a slipping plane where there is an interface between a stationary layer of fluid attached to the particle and the dispersion medium [Hunter 1988]. A colloidal suspension is considered to be electrostatically stable if the zeta potential is either greater than 20 mV or smaller than -20 mV.

The measured values of zeta potential between different batches varied between -26.5 mV and -7 mV. For the batches with zeta potential between -20 mV and -7 mV, the NP solution was stable in water mostly because of steric repulsion rather than electrostatic repulsion. Most likely the hydrophilic chains of TREG associated with water molecules, thus preventing agglomeration.

2.2.2 *Thermogravimetric analysis.* Thermogravimetric analysis and differential scanning calorimetry (TGA/DSC) are complementary techniques to investigate material's response to different temperatures: mass change (for example, decomposition or sublimation temperatures) and thermal changes often unaccompanied by the mass change as a function of temperature (e.g., melting, glass transition, heat capacity, enthalpy, and second-order phase transitions). We have used Netzsch STA 449 F1 Jupiter apparatus to determine mass fraction of the as-synthesized NPs that can be attributed to the Fe<sub>3</sub>O<sub>4</sub> material, as opposed to organic TREG coating.

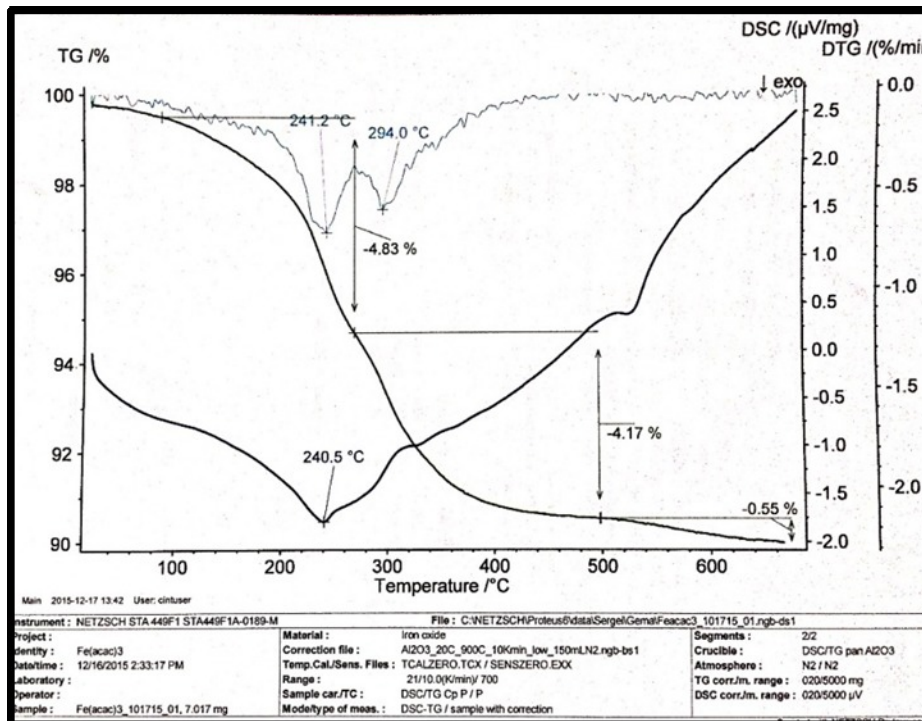


Fig. 5. Results of TGA and DSC analysis of Fe<sub>3</sub>O<sub>4</sub>/TREG NPs.

The TGA results displayed in Fig. 5 indicate that ~10% of the mass of as-synthesized NPs was due to the organic coating. The onset of initial decomposition of TREG is 240 °C, consistent with an increased rate of loss of mass at 240.5 °C shown in Fig. 5.

### 2.3 Determination of Reaction Yield

The reaction yield was determined as follows. First, the amount of Fe(acac)<sub>3</sub> precursor added to the reaction flask was carefully weighed and converted into the initial number of moles of iron. Then, the weight of each empty scintillation vial was recorded, and compared with the weight of the same vials filled with the NP powder. The net difference was further reduced by 10%, based on the results of thermogravimetric analysis. The resultant weight of Fe<sub>3</sub>O<sub>4</sub> NPs was then converted into the final number of moles of iron. The ratio of the final and initial numbers of moles of irons was taken as the reaction yield. In the particular case of the reaction described in Section 2.1, the reaction yield was 82.5%. In other batches, yields as high as 93% were obtained.

## 3. METHODOLOGY OF BACTERIAL BIOFILM INVESTIGATIONS

### 3.1 Methods

3.1.1 *Microbial inocula.* Unstimulated whole saliva was collected from a healthy adult male and stored at -80 °C until further use. Microbial growth medium was prepared in brain-heart infusion medium supplemented with 6% (v/v) sheep blood. Immediately prior to each experiment, whole saliva from the stock was added to growth medium to prepare mixed-species oral microbial suspension (10% (v/v) saliva in the final suspension).

**3.1.2 Biofilm formation.** Mixed species oral biofilms were developed as described in [Bandara 2010a] and [Martin 2012] with the following modifications. Commercially available pre-sterilized, polystyrene, flat bottom 6-well microtiter plates (BD Biosciences, California, USA) were used. At first, 3 mL of microbial suspension were transferred into the wells of a microtiter plate, and the plate was incubated for 24 h (37 °C, 75 rpm) under aerobic growth conditions. At the end of the incubation, wells were washed twice with PBS to eliminate traces of the medium and free-floating microbial cells. The effects of various treatments were studied on such preformed biofilms over a period of 24 h.

### 3.2 Determination of Concentration-Dependent Effects of Fe<sub>3</sub>O<sub>4</sub> Nanoparticles

**3.2.1. Biofilm phase.** Mixed species oral biofilms were developed in sterile 96-well plates (BD Biosciences, USA) as described above. Biofilms were washed twice with PBS and Fe<sub>3</sub>O<sub>4</sub> NPs were administered in a concentration gradient (two fold). The plates were incubated for 24 h at 37 °C.

At the end of the incubation period, XTT reduction assay (2,3,-bis(2-methoxy-4-nitro-5-sulfophenyl)-2H-tetrazolium-5-carboxanilide) from Thermo Fisher Scientific was performed to quantify the viability of biofilms. The assay was performed in quadruplicates at two times.

**3.2.2. Biofilm formation and treatment.** Mixed species oral biofilms were developed for 24 h in sterile 6-well plates as described above. 24-h biofilms were washed twice with sterile phosphate buffered saline (PBS) and the NPs suspended in PBS (200µg/ml) were administered onto mixed-species oral biofilms. Biofilms that were untreated with NPs were used as controls. Subsequently, the plates were exposed to one of two different magnetic field treatments. Static magnetic field treatments involved exposing the 24-h biofilm, with or without NPs, to magnetic fields from the bottom of the 6-well plate for 6 h using molybdenum magnets (magnetic field strength at the biofilm = 4.44 kGs, Fig. 6(a)). Switched static magnetic field treatment involved exposing the 24-h biofilm, with or without NPs, to magnetic fields from the bottom of the 6-well plates for 30 min (magnetic field strength = 4.44 kGs), followed by exposing from the top of the 6-well plate for 30 min (magnetic field strength was reduced to 0.12 kGs) for 6 h of total exposure (Fig. 6(b)). After magnetic field treatment, biofilms were incubated in an incubator for 24 h at 37 °C. At the end of incubation period, the biofilms were washed twice with PBS, and the XTT reduction assay was performed to quantify the viability of biofilms by means of measuring their metabolic activity.

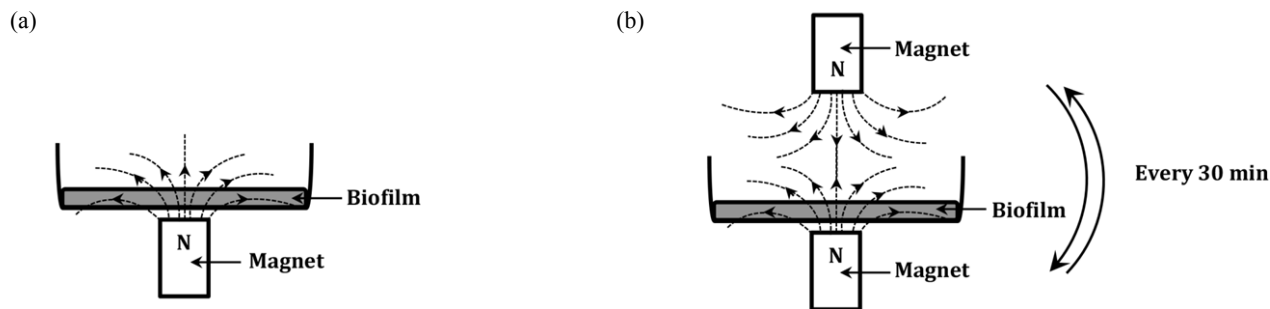


Fig. 6. Methods of mixed species oral biofilm exposure to different magnetic fields. (a) Static one-sided magnetic field exposure. Magnets were placed under the 6-well plates for 6 h. (b) Static switched magnetic field exposure. The locations of the magnets were switched from top to bottom and vice versa every 30 min for 6 h.

**3.2.3 XTT reduction assay.** At the end of incubation of both test and control biofilms, a standard XTT (sodium 2,3,-bis(2-methoxy-4-nitro-5-sulfophenyl)-5-[(phenylamino)-carbonyl]-2H-tetrazolium inner salt) reduction assay from ATCC was performed thereafter, as described in [Bandara 2010b], to measure the viability of biofilms by means of bacterial cell metabolic activity. In brief, commercially available XTT powder (Sigma, MO, USA) was dissolved in PBS to a final concentration of 1 mg/mL. Then the solution was filter-sterilized (0.22 µm pore size filter) and stored at -70 °C. Freshly prepared 0.4 mM menadione solution was used for XTT reduction assay. XTT solution was thawed and mixed with menadione solution at 20:1 (v/v) immediately before the assay. Thereafter, PBS:XTT:menadione in 79:20:1 proportion were added into each culture dish containing biofilms and incubated in the dark for 5 h at 37 °C. The color changes were measured with a microtiter plate reader (Infinite M200 microplate reader, TECAN US Inc, NC, USA) at 492 nm. All assays were carried out in triplicate on two different occasions.

3.2.4. *Confocal laser scanning microscopy.* Biofilms were prepared on sterile cover slips placed in commercially available sterile flat bottom 6-well plates (Nunclon, Nunc, Thermo Fisher Scientific, USA) as described above. Pre-formed 24-h biofilms were exposed to magnetic fields with or without NPs and incubated for another 24 h at 37 °C. At the end of incubation, the prewashed coverslips were stained with Live and Dead stain (Live/Dead BacLight Bacterial Viability kit, Invitrogen, Eugene, USA) [Bandara 2010a]. The biofilm was then analyzed by fluorescent microscopy (using a confocal laser scanning microscope, Nikon C2 inverted confocal microscope, Nikon, Japan).

3.2.5. *Statistical analysis.* Statistical analysis was performed using the SPSS software (version 16.0). Mann-Whitney U-test was performed to compare the significant differences between the corresponding control and test samples of the mixed-species oral biofilms and to compare the significant differences between test samples of the mixed-species oral biofilms under different treatment conditions. A *P*-value of less than 0.05 was considered statistically significant.

## 4. RESULTS OF BACTERIAL BIOFILM INVESTIGATIONS

### 4.1 Effects of Magnetic Fields on Mixed-Species Oral Biofilms Treated with Control Particles

4.1.1. *Biofilm metabolism (XTT reduction assay).* When the biofilms were treated with various magnetic fields as mentioned above, all test samples exposed to magnetic fields exhibited significant reduction in the metabolic activity compared to untreated (*i.e.* magnetic-field free) biofilm controls (*P* < 0.05, Table 1 and Fig. 7(a)). Comparing the different magnetic field treatments to each other, no significant differences in the mean XTT readings were found.

Table 1: Metabolic activities (XTT) of mixed species oral biofilms exposed to NP treatment and magnetic fields  
*P* < 0.05 is considered statistically significant

Treatment group	Mean XTT±SD	% reduction compared to control	<i>P</i> value (compared to control)
Control	0.452±0.046		
Static one sided only	0.320±0.031	29	< 0.05
Static switched only	0.263±0.024	42	< 0.05
NPs only	0.300±0.009	34	< 0.05
NPs + Static one sided	0.207±0.024	54	< 0.05
NPs + Static switched	0.213±0.018	53	< 0.05

4.1.2. *Confocal laser scanning microscopy.* The control biofilm (Fig. 8(a)) that was not exposed to magnetic fields demonstrated a dense, spatially oriented and confluent biofilm, with substantial amount of extracellular substances for 24-h biofilms. In contrast, the biofilms exposed to both one-sided and switched static magnetic fields exhibited significantly lower quantity of microbial cells and lack of organized structure or extracellular substances (Figs. 8(b) and 8(c)). Few isolated microbial colonies were seen in the biofilm after static one-sided exposure, whereas scattered smaller microbial colonies were observed when treated with static switched magnetic fields.

### 4.2. Effects of Various Magnetic Fields on Mixed-Species Oral Biofilms Co-treated with Fe<sub>3</sub>O<sub>4</sub> Nanoparticles

4.2.1. *Concentration-dependent effect of NPs on mixed-species oral biofilms.* When treated with NPs at concentrations above 8 µg/mL, mixed oral biofilms showed 26-34% reduction in the metabolism as indicated by XTT readings (Fig. 7(c)).

4.2.2. *Biofilm metabolism (XTT reduction assay).* When the biofilms treated with NPs were exposed to aforementioned different magnetic fields, all test treatments showed significant suppression of biofilm metabolism (*P* < 0.05) compared to untreated biofilm control as well as NP-treated biofilms (Table 1 and Fig. 7(b)). Biofilms that were exposed to NPs alone had a significantly lowered metabolic activity compared to control biofilms (*P* < 0.05, Figure 2B, Table 1). Comparing the different magnetic field treatments to each other, no significant differences in the mean XTT readings were found (Table 1).

4.2.3. *Confocal laser scanning microscopy.* When treated with NPs, oral biofilms showed a significantly lower biofilm mass compared to controls (Fig. 8(d)). More importantly, there was a notable reduction in the extracellular matrix in the biofilms treated with NPs (Fig. 8(d) vs. Fig. 8(a)). However, the remnants of the biofilm structure were preserved. When the biofilms treated with NPs were exposed to either static one-sided or static switched magnetic fields, complete

destruction of the biofilms was noted (Figs. 8(e) and 8(f)). There was no structured biofilm or extracellular matrix observed in confocal laser scanning microscopy images. Instead, scattered bacterial cells were visible in the microscopic field compared to the control biofilm (Figs. 8(e) and 8(f)).

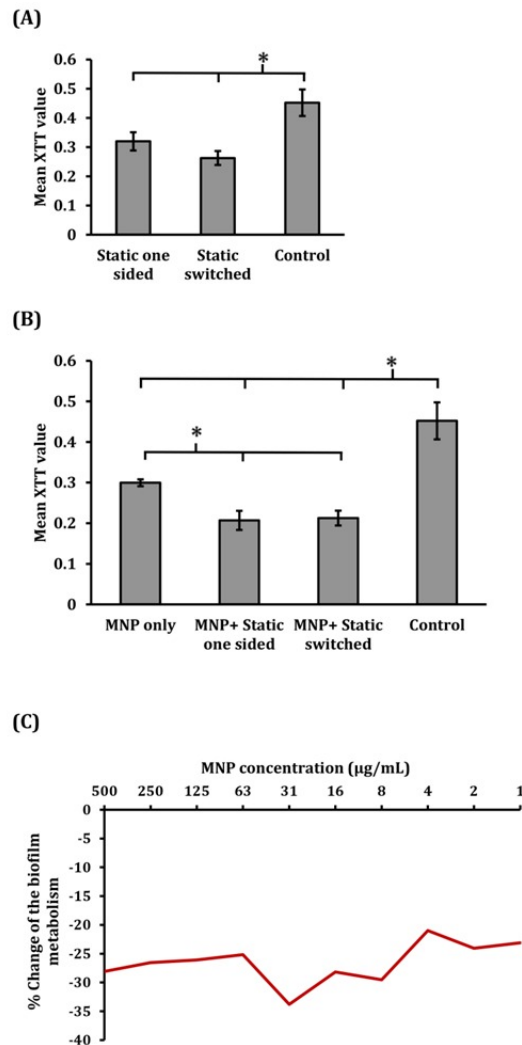


Fig. 7. A composite figure of the metabolic activities (XTT) of mixed species oral biofilms exposed to NP treatment and magnetic fields. (a) Biofilms only with magnetic exposure; note the significantly lower metabolic activity of the biofilm exposed to both static one-sided and static switched magnetic fields compared to unexposed controls. \* indicates significant changes and  $P < 0.05$  is considered statistically significant. (b) Biofilms treated with NPs (200 µg/mL) and exposed to static magnetic fields; note the significantly lower metabolic activities of the biofilms treated with NPs compared to controls and treated with NPs and exposed to magnetic fields compared to both controls and biofilms treated only with NPs. (c) The concentration-dependent effect of NPs on preformed 24-h mixed-species oral biofilms; The biofilm metabolic activity was suppressed between 26-34% when treated with more than 8 µg/mL of NPs.

It should be noted that our results are consistent with a recent report of synergistic antimicrobial effect of a static magnetic field and hydroxyapatite/iron oxide ferromagnetic nanocomposite substrates on *Staphylococcus aureus* and *Escherichia coli* [Bajpai 2014].

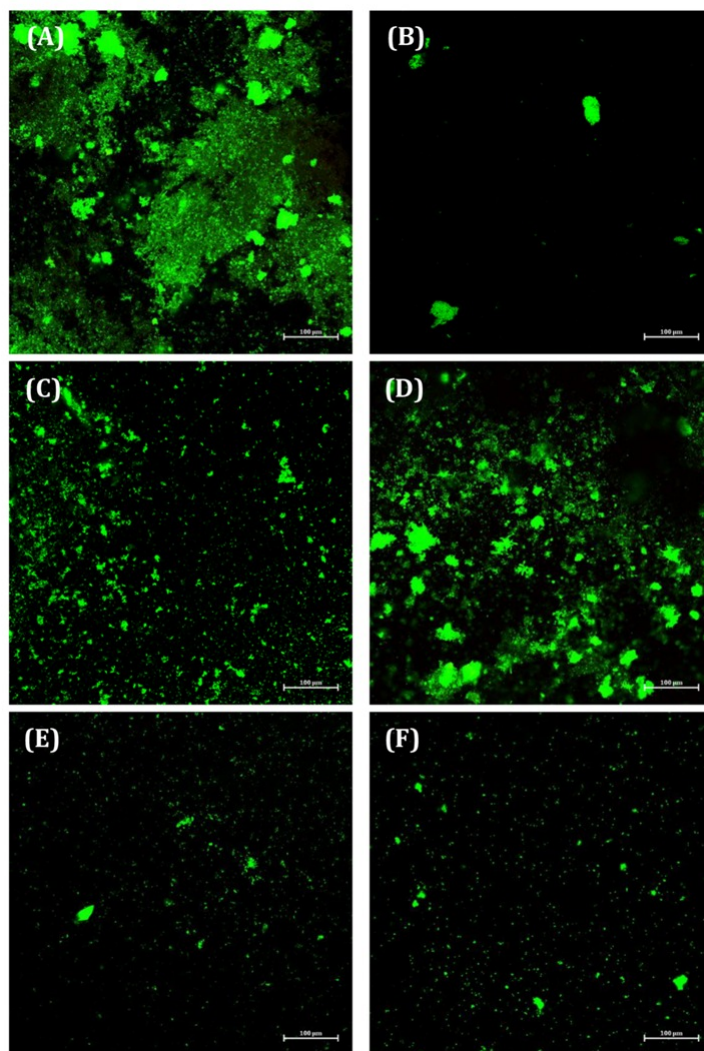


Fig. 8. Confocal laser scanning microscopy images of mixed-species oral biofilms exposed to different magnetic fields with or without NP treatment (magnification  $\times 20$ ) (stained using a LIVE/DEAD BacLight bacterial viability kit; Invitrogen); Live cells are stained in green and dead cells in red. The absence of red-stained cells indicates that while the biofilms were disrupted, the bacteria cells were not killed. (a) Undisturbed control. (b) Biofilm exposed to static one-sided magnetic fields. (c) Biofilm exposed to static switched magnetic fields. (d) Biofilm exposed to NPs (200  $\mu\text{g}/\text{mL}$ ) alone. (e) Biofilm exposed to NPs and static one-sided magnetic fields. (f) Biofilm exposed to NPs and static switched magnetic fields. Note the significant reduction of the cellular content, stratified architecture, and lack of extracellular components in the test biofilms (b) through (f) compared to three-dimensionally arranged and dense biofilm controls with substantial extracellular materials (a).

## 5. ACKNOWLEDGEMENTS

The authors wish to express their gratitude to Dr. Ricardo H. Gonçalves from Laboratório de Nanocaracterização, Universidade Federal de São Carlos, Brazil, for useful discussions. This work was performed, in part, at the Center for Integrated Nanotechnologies, an Office of Science User Facility operated for the U.S. Department of Energy (DOE) Office of Science by Los Alamos National Laboratory and Sandia National Laboratories (Contract DE-AC04-94AL85000). Los Alamos National Laboratory, an affirmative action equal opportunity employer, is operated by Los Alamos National Security, LLC, for the National Nuclear Security Administration of the U.S. Department of Energy under contract DE-AC52-06NA25396. Sandia National Laboratories is a multi-program laboratory managed and operated by Sandia Corporation, a wholly owned subsidiary of Lockheed Martin Corporation, for the U.S. Department of Energy's National Nuclear Security Administration under contract DE-AC04-94AL85000.

## 6. REFERENCES

- [Arakha 2015] M. Arakha, S. Pal, D. Samantarrai, T. K. Panigrahi, B. C. Mallick, K. Pramanik, B. Mallick, and S. Jha, "Antimicrobial activity of iron oxide nanoparticle upon modulation of nanoparticle-bacteria interface", *Scientific Reports*, vol. 5, Art. 14813 (12+4 pp.), 6 Oct. 2015.
- [Armijo 2015] L. M. Armijo, P. Jain, A. Malagodi, F. Z. Fornelli, A. Hayat, A. C. Rivera, M. French, H. D. C. Smyth, and M. Osiński, "Inhibition of bacterial growth by iron oxide nanoparticles with and without attached drug: Have we conquered the antibiotic resistance problem?", *Colloidal Nanoparticles for Biomedical Applications X* (W. J. Parak, M. Osiński, and X.-J. Liang, Eds.), SPIE International Symposium on Biomedical Optics BiOS 2015, San Francisco, CA, 7-9 Feb. 2015, *Proceedings of SPIE*, vol. 9338, Paper 1Q (11 pp.).
- [Bajpai 2014] I. Bajpai, K. Balani, and B. Basu, "Synergistic effect of static magnetic field and HA-Fe<sub>3</sub>O<sub>4</sub> magnetic composites on viability of *S. aureus* and *E. coli* bacteria", *Journal of Biomedical Materials Research Part B: Applied Biomaterials*, vol. 102B, pp. 524-532, April 2014.
- [Bandara 2010a] H. M. H. N. Bandara, J. Y. Y. Yau, R. M. Watt, L. J. Jin, and L. P. Samaranayake, "Pseudomonas aeruginosa inhibits in-vitro Candida biofilm development", *BMC Microbiology*, vol. 10, Art. 125 (9 pp.), April 2010.
- [Bandara 2010b] H. M. H. N. Bandara, O. L. T. Lam, R. M. Watt, L. J. Jin, and L. P. Samaranayake, "Bacterial lipopolysaccharides variably modulate in vitro biofilm formation of Candida species", *Journal of Medical Microbiology*, vol. 59, pp. 1225-1234, 2010.
- [Behera 2012] S. S. Behera, J. K. Patra, K. Pramanik, N. Panda, and H. Thatoi, "Characterization and evaluation of antibacterial activities of chemically synthesized iron oxide nanoparticles", *World Journal of Nano Science and Engineering*, vol. 2, pp. 196-200, Dec. 2012.
- [Cai 2007] W. Cai and J. Q. Wan, "Facile synthesis of superparamagnetic magnetite nanoparticles in liquid polyols", *Journal of Colloid and Interface Science*, vol. 305, pp. 366-370, 2007.
- [Carrouel 2016] F. Carrouel, S. Viennot, J. Santamaria, P. Veber, and D. Bourgeois, "Quantitative molecular detection of 19 major pathogens in the interdental biofilm of periodontally healthy young adults", *Frontiers in Microbiology*, vol. 7, Art. 840 (16 pp.), June 2016.
- [Chen 2014] Z. J. Chen, Y. Wang, T. Ba, Y. Li, J. Pu, T. Chen, Y. S. Song, Y. E. Gu, Q. Qian, J. L. Yang, and G. Jia, "Genotoxic evaluation of titanium dioxide nanoparticles in vivo and in vitro", *Toxicology Letters*, vol. 226 (#3), pp. 314-319, May 2014.
- [Coccini 2015] T. Coccini, S. Grandi, D. Lonati, C. Locatelli, and U. De Simone, "Comparative cellular toxicity of titanium dioxide nanoparticles on human astrocyte and neuronal cells after acute and prolonged exposure", *NeuroToxicology*, vol. 48, pp. 77-89, May 2015.
- [Czajka 2015] M. Czajka, K. Sawicki, K. Sikorska, S. Popek, M. Kruszewski, and L. Kapka-Skrzypczak, "Toxicity of titanium dioxide nanoparticles in central nervous system", *Toxicology in Vitro*, vol. 29 (#5), pp. 1042-1052 Aug. 2015.
- [Darwish 2015] M. S. A. Darwish, N. H. A. Nguyen, A. Ševců, and I. Stibor, "Functionalized magnetic nanoparticles and their effect on *Escherichia coli* and *Staphylococcus aureus*", *Journal of Nanomaterials*, vol. 2015, Art. 416012 (10 pp.), 2015.
- [Eke 2012] P. I. Eke, B. A. Dye, L. Wei, G. O. Thornton-Evans, and R. J. Genco, "Prevalence of periodontitis in adults in the United States: 2009 and 2010", *Journal of Dental Research*, vol. 91 (#10), pp. 914-920, 2012.
- [Filoche 2010] S. Filoche, L. Wong, and C. H. Sissons, "Oral biofilms: Emerging concepts in microbial ecology", *Journal of Dental Research*, vol. 89 (#1), pp. 8-18, 2010.
- [Gonçalves 2010] R. H. Gonçalves, C. A. Cardoso, and E. R. Leite, "Synthesis of colloidal magnetite nanocrystals using high molecular weight solvent", *Journal of Materials Chemistry*, vol. 20 (#6), pp. 1167-1172 (2010).
- [Hong 2015] F. S. Hong, L. Sheng, Y. G. Ze, J. Hong, Y. J. Zhou, L. Wang, D. Liu, X. H. Yu, B. Q. Xu, X. Y. Zhao, and X. Ze, "Suppression of neurite outgrowth of primary cultured hippocampal neurons is involved in impairment of glutamate metabolism and NMDA receptor function caused by nanoparticulate TiO<sub>2</sub>", *Biomaterials*, vol. 53, pp. 76-85, June 2015.
- [Garcia-Contreras 2015] R. Garcia-Contreras, M. Sugimoto, N. Umemura, M. Kaneko, Y. Hatakeyama, T. Soga, M. Tomita, R. J. Scougall-Vilchis, R. Contreras-Bulnes, H. Nakajima, and H. Sakagami, "Alteration of metabolomic profiles by titanium dioxide nanoparticles in human gingivitis model", *Biomaterials*, vol. 57, pp. 33-40, July 2015.

- [Hanot-Roy 2016] M. Hanot-Roy, E. Tubeuf, A. Guilbert, A. Bado-Nilles, P. Vigneron, B. Trouiller, A. Braun, and G. Lacroix, "Oxidative stress pathways involved in cytotoxicity and genotoxicity of titanium dioxide (TiO<sub>2</sub>) nanoparticles on cells constitutive of alveolo-capillary barrier *in vitro*", *Toxicology in Vitro*, vol. 33, pp. 125-135, June 2016.
- [Hunter 1988] R. J. Hunter, *Zeta Potential in Colloid Science: Principles and Applications*, Academic Press, 1988.
- [Iavicoli 2016] I. Iavicoli, L. Fontana, and G. Nordberg, "The effects of nanoparticles on the renal system", *Critical Reviews in Toxicology*, vol. 46 (#6), pp. 490-560, 2016.
- [Khan 2015] M. Khan, A. H. Naqvi, and M. Ahmad, "Comparative study of the cytotoxic and genotoxic potentials of zinc oxide and titanium dioxide nanoparticles", *Toxicology Reports*, vol. 2, pp. 765-774, 2015.
- [Kolenbrander 2002] P. E. Kolenbrander, R. N. Andersen, D. S. Blehert, P. G. Eglund, J. S. Foster, and R. J. Palmer Jr., "Communication among oral bacteria", *Microbiology and Molecular Biology Reviews*, vol. 66 (#3), pp. 486-505, Sept. 2002.
- [Kongseng 2016] S. Kongseng, K. Yoovathaworn, K. Wongprasert, R. Chunhabundit, P. Sukwong, and D. Pissuwan, "Cytotoxic and inflammatory responses of TiO<sub>2</sub> nanoparticles on human peripheral blood mononuclear cells", *Journal of Applied Toxicology*, vol. 36 (#10), pp. 1364-1373, Oct. 2016.
- [Martin 2012] G. C. Martin, *Development of an Orally Relevant Biofilm Disinfection Model*, Ph.D. Dissertation, University College London, UK, 2012 (660 pp.).
- [Niemirowicz 2015] K. Niemirowicz, U. Surel, A. Z. Wilczewska, J. Mystkowska, E. Pikel, X. B. Gu, Z. Namiot, A. Kułakowska, P. B. Savage, and R. Bucki, "Bactericidal activity and biocompatibility of ceragenin-coated magnetic nanoparticles", *Journal of Nanobiotechnology*, vol. 13, Art. 32 (11 pp.), 1 May 2015.
- [Prabhu 2015] Y. T. Prabhu, K. V. Rao, B. S. Kumari, V. S. S. Kumar, and T. Pavani, "Synthesis of Fe<sub>3</sub>O<sub>4</sub> nanoparticles and its antibacterial application", *International Nano Letters*, vol. 5, pp. 85-92, 2015.
- [Rudramurthy 2016] G. R. Rudramurthy, M. K. Swamy, U. R. Sinniah, and A. Ghasemzadeh, "Nanoparticles: Alternatives against drug-resistant pathogenic microbes", *Molecules*, vol. 21 (#7), Art. 836 (30 pp.), 2016.
- [Schmid 2016] O. Schmid and T. Stoeger, "Surface area is the biologically most effective dose metric for acute nanoparticle toxicity in the lung", *Journal of Aerosol Science*, vol. 99, Special Issue, pp. 133-143, Sept. 2016.
- [Tran 2010] N. Tran, A. Mir, D. Mallik, A. Sinha, S. Nayar, and T. J. Webster, "Bactericidal effect of iron oxide nanoparticles on *Staphylococcus aureus*", *International Journal of Nanomedicine*, vol. 5, pp. 277-283, 2010.
- [Von Hoene 1958] J. Von Hoene, R. G. Charles, and W. M. Hickam, "Thermal decomposition of metal acetylacetonates. Mass spectrometer studies", *Journal of Physical Chemistry*, vol. 62 (#9), pp. 1098-1101, Sept. 1958.